

SIMPRO, SPACE DEBRIS SIMULATOR AND PROPAGATION - USER GUIDE

MARIUS APETRII, ALESSANDRA CELLETTI, CHRISTOS
EFTHYMIPOULOS, CĂTĂLIN GALEȘ, AND TUDOR VARTOLOMEI

CONTENTS

1. Introduction	2
2. Quick description of the main menu	3
3. Option 1: generate a single break-up event	4
3.1. Work-flow	4
3.2. Choosing Orbital Elements	4
3.3. Collisions options	5
3.4. Explosions options	5
3.5. Fragments' propagation	6
3.6. Setting equations' parameters	6
3.7. Output	7
3.8. Save Experiment	10
4. Option 2: generate multiple break-up events	13
4.1. Work-flow	13
4.2. Choosing Orbital Elements	13
4.3. Number and Distance between Events	13
4.4. Fragments' propagation	14
4.5. Output	15
5. Option 3: Saved experiments	16
6. Option 4: Orbits' propagator	17
6.1. Workflow	17
6.2. Choosing Orbital Elements	18
6.3. Selecting the framework	18
6.4. Selecting the forces	19
6.5. Choosing the integration time and step	19
6.6. Choosing the integration method	19
6.7. Output	20
6.8. Propagation history	20
7. Option 5: User guide page	22
8. Option 5: Copyright page	23
9. Option 6: Reload application button	24
References	24

I. INTRODUCTION

SIMPRO is a space debris simulator of break-up events, based on NASA's model EVOLVE 4.0 ([3], see also [1]); it also allows to propagate the orbits using different formalisms (Cartesian or Hamiltonian). SIMPRO represents a useful tool in the analysis of satellites and space debris dynamics, with the aim to provide information on break-up events, either collisions or explosions, and their subsequent dynamics. The application is written in JAVA and can be executed on a wide set of operating systems.

These guidelines are intended to give the user basic information to run the program; details can be found in the accompanying paper [2].

The executable program is publicly available and it can be downloaded from the following link:

SIMPRO GitHub repository

IMPORTANT NOTE: When using the results of this simulator in articles, books, videos, or any other mean, acknowledge the use making reference to:

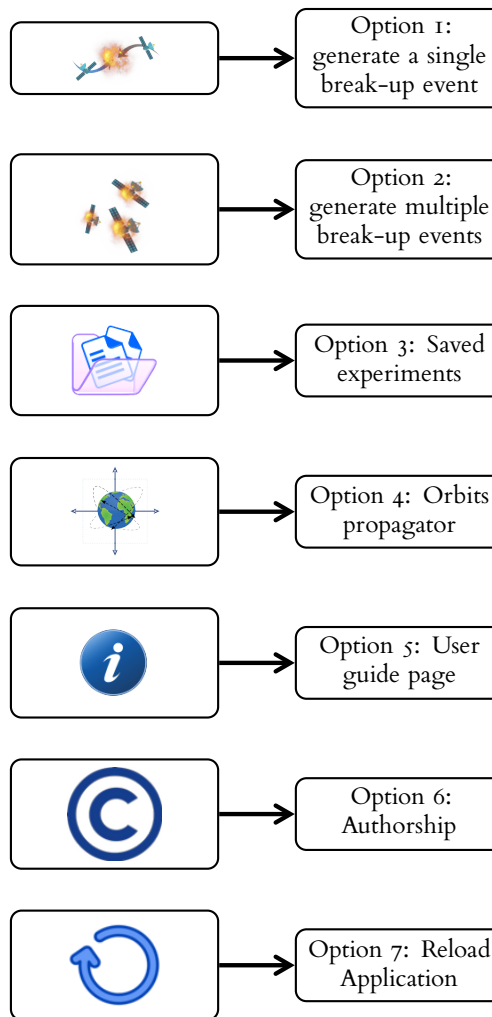
M. Apetrii, A. Celletti, E. Efthymiopoulos, C. Gales, T. Vartolomei, *Simulating a breakup event and propagating the orbits of space debris*, *Celestial Mechanics and Dynamical Astronomy* 136 (5), 35 (2024).

Any question on SIMPRO can be addressed on GitHub or writing to:
simpro.project@gmail.com

Refer to these notes as: Version 1.0 - September 2024.

2. QUICK DESCRIPTION OF THE MAIN MENU

This section reproduces the left column that appears when opening SIMPRO and explains the meaning of the symbols, which correspond to the different options that the user can select. The following sections will provide further details on each option.

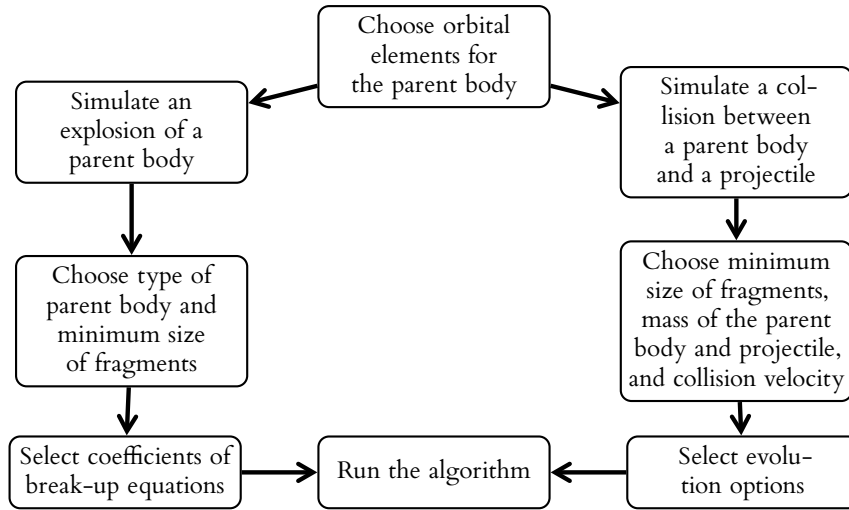


3. OPTION 1: GENERATE A SINGLE BREAK-UP EVENT

The first option of SIMPRO reproduces the break-up model Evolve 4.0 provided by NASA for a single break-up event.

It allows one to determine the cross-sections, masses, and imparted velocities of the fragments after an explosion or a collision. Section 3.1 describes the work-flow, Section 3.2 illustrates how to choose the initial orbital elements, Sections 3.3 and 3.4 explain, respectively, the procedure to simulate a collision or an explosion, Section 3.5 shows how to get the evolution of each fragment on a given time interval, Section 3.6 explains how to change some settings with respect to [3], Section 3.7 describes the different outputs generated by SIMPRO, Section 3.8 shows how to save the data of an experiment.

3.1. Work-flow. The work-flow of SIMPRO is illustrated below.



3.2. Choosing Orbital Elements. Choose Mean elements (TLE) and provide the orbital elements of the parent body (where the break-up event will happen).

- Semi-major axis in km: $a > 6400$ km and $a < 45000$ km.
- Eccentricity $e \in [0, 0.75]$.
- Inclination in degrees: $i \in [0, 180^\circ]$.
- Mean anomaly in degrees: $M \in [0, 360^\circ]$.
- Argument of perigee in degrees: $\omega \in [0, 360^\circ]$.
- Argument of the ascending node in degrees: $\Omega \in [0, 360^\circ]$.

An example is given in Figure 1.

Parent Body Position	
Mean Elements (TLE)	Two Line Elements
Semi-major axis [km]	21600
Eccentricity	0.1
Inclination [°]	63.5
Mean anomaly [°]	80
Argument of perigee [°]	70
Longitude of the ascending node [°]	60

FIGURE 1. Orbital Elements of Parent Body.

Alternatively, choose **Two Line Elements** and provide the data in LINE 1 and LINE 2 using the NORAD format from CelesTrak.

3.3. Collisions options.

- Choose the size of the smallest fragment generated, with the constraint ≥ 1 cm.
- Set the masses of parent body between 300 and 15 000 kg.
- Set the masses of parent body between 0.001 and 5 kg.
- Choose the impact velocity between 1 and 10 000 m/s.
- Select the type of parent body: **Drop down menu** **Upper Stage** or **Drop down menu** **Spacecraft**

An example is given in Figure 2.

The "Output" frame gives the number of generated fragments and the number of fragments with elliptic orbits, taking into account that some fragments can fall on the Earth. Besides, it gives "Catastrophic: false" or "Catastrophic: true", the latter case occurring whenever the energy of break-up is greater than 40 kJ, which means that the parent body is completely disintegrated. This could happen only in case of a collision with a heavy projectile at a high relative velocity.

3.4. Explosions options. After having chosen the mean elements of the parent body as in Section 3.3, proceed to fix the parameters of break-up.

FIGURE 2. Collision options.

- Choose the size L_c of the smallest fragment generated, with the constraint ≥ 1 cm.
- Select the type of parent body:

Drop down menu >> Molniya Satellite | Ukrainian Tsyklon | Soviet Antisatellite | Soviet Battery

Drop down menu (continued) >> Soviet Eorsat | Regular Body | Titan Transtage

The "Output" frame gives the number of generated fragments and the number of fragments with elliptic orbits, taking into account that some fragments can fall on the Earth.

3.5. Fragments' propagation. To activate the propagation of the fragments, select **Toggle activation** with a LEFT CLICK and set the options with a RIGHT CLICK. One can choose "short-term" and "long-term" propagation, providing the period and step, the initial time and selecting the forces one wants to include in the propagation, namely the J_2 and J_3 terms of the geopotential, the effects of Moon and Sun, the Solar radiation pressure, and the drag effect due to the Earth's atmosphere, see Figure 3.

3.6. Setting equations' parameters. You may change the original coefficients and parameters of the NASA Evolve 4.0 equations described in [1], [3], see Figure 5.

- Open the pop-up window by pressing **Set Parameters - More Info** button.

FIGURE 3. Options for the propagation of each fragment for a period of time.

FIGURE 4. Set NASA Evolve 4.0 parameters.

- Find the equation you want to modify and set the value of the parameter(s) within the editable boxes. The boxes provide the default values; a pop-up window that opens passing on the editable boxes provides the allowed intervals for each parameter.
- You may change one or more parameters.
- Save your choice parameters using `Save and close` button on top of the window.

Notice that a slightly change in the NASA Evolve 4.0 parameters could give major differences in the results. Please refer to [1] and [2] for more details

3.7. Output. The output panel has two different frameworks, according to whether the orbits are propagated or not.

3.7.1. Orbital Elements Plots. The orbital elements a , e , i are plotted in the 2-dimensional planes of $a - i$, $a - e$, and $e - i$; Figure 6 shows the output without (left panel) and with propagation of the orbits (right panel).

3.7.2. Data Analysis. It provides a statistical analysis of the data after a break-up event by computing mean, median, min, max, range, variance, standard deviation, mean standard error, coefficient of variation of the orbital elements, size, area-to mass ratio and velocity distributions. Figure 7 shows the output after a propagation.

The output in Figure 7 is described as follows:

Save and Close

2. NUMBER OF EXPLOSION OR COLLISION FRAGMENTS

Given a characteristic length, say $L_c = \frac{1}{3}(L_x + L_y + L_z)$ as the average of the principal geometric axis of the fragment, the cumulative number of explosion or collision fragments N_{frag} of diameter $d \geq L_c$ can be determined as

$$N_{frag}(d \geq L_c) = 6 \cdot S \cdot \hat{L}_c^{p_c}, \quad \text{for explosion}$$

$$N_{frag}(d \geq L_c) = 0.1 \cdot \hat{M}^{0.75} \cdot \hat{L}_c^{p_c}, \quad \text{for collisions}$$

If you want to change the default value for p_c (-1.6), please insert it in the next field.

-1.6

If you want to change the default value for p_c (-1.71), please insert it in the next field.

-1.71

S is a scaling parameter, $0.1 \leq S \leq 2$ with:

- $S = 0.1$ for Soviet/Russian proton ullage motor, Molniya satellite,
- $S = 0.25$ for Ukrainian Tsyklon third stage,
- $S = 0.3$ for Soviet anti-satellite,
- $S = 0.5$ for Soviet battery related explosion,
- $S = 0.6$ for Soviet EORSAT,
- $S = 1$ for regular/rocket body,
- $S = 2$ for Titan transtage.

The hat in the notation denotes normalized quantities:

$$\hat{L}_c = L_c/[m]$$

and

$$\begin{aligned} \hat{M} &= m_t + m_p/[kg] & \text{for } \hat{E}_p \geq \hat{E}_p^* \\ \hat{M} &= \frac{m_p v_i}{1000}/[kg \text{ ms}^{-1}] & \text{for } \hat{E}_p < \hat{E}_p^* \end{aligned} \quad (2.2)$$

with $\hat{E}_p = \frac{1}{2} \frac{m_p}{m_t} v_i^2$, $\hat{E}_p^* = 40/[kJ \text{ kg}^{-1}]$, m_t is the mass of a collision target object (spacecraft or upper stage), m_p is the mass of an impact projectile, v_i is the impact velocity. \hat{E}

FIGURE 5. Set parameters window

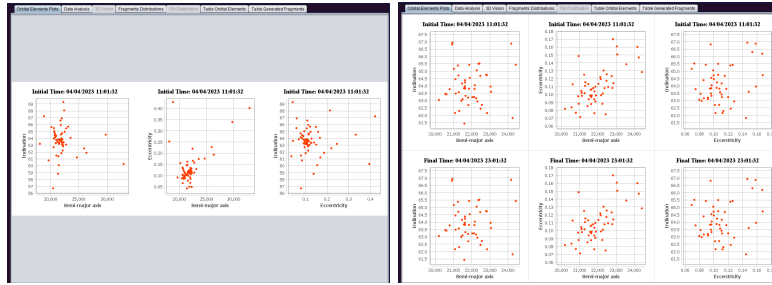


FIGURE 6. Orbital elements plots.

- First row: statistics at break-up time;
- Second row: histograms of a , e , i at break-up;
- Third row: histograms of a , e , i after evolution period;
- Forth row: statistics after evolution period.

3.7.3. *3D Orbit Vision*. This page allows to visualize the position of the generated fragments in a 3-dimensional space, whenever the propagation

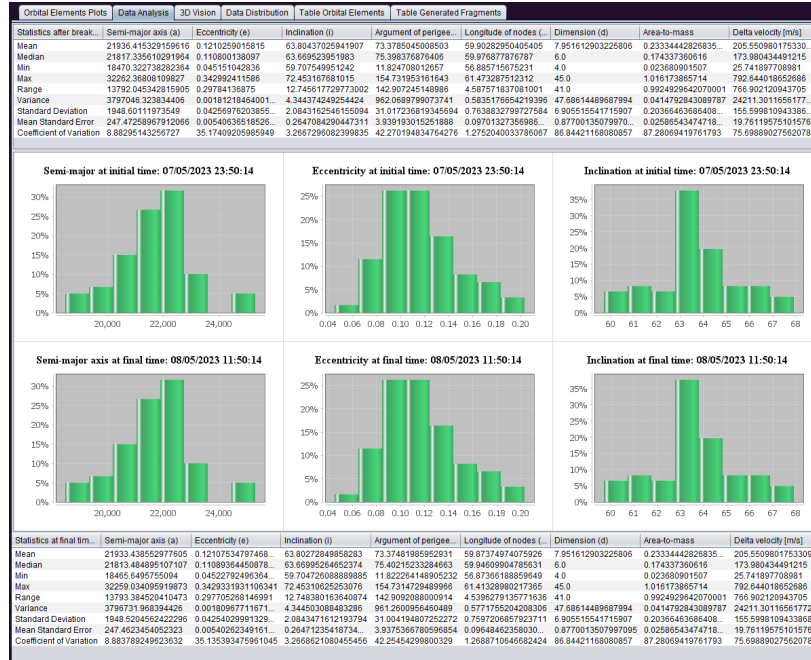


FIGURE 7. Data analysis window.

has been computed. An example is given in Figure 8 with the following description, where the blue dots make the contour plot of the Earth surface:

- Top-left: parent body position at break-up time.
- Top-right: fragments' orbits after one fourth of period.
- Bottom-left: fragments' position after three fourths of period.
- Bottom-right: fragments' orbits at final time.

Each panel has additional options to zoom and move the graphs, rotate the plot, reset the zoom, modify the scale settings, save the picture, have a list of Cartesian coordinates (X, Y, Z) of each fragment at a given time, the coordinates of the parent body that gives the orbit, the coordinates of the blue dots representing the Earth. An option allows one to decide whether visualize the fragments, parent body, and the Earth.

3.7.4. Data Distribution. This page shows the ξ -distribution described in the NASA model ([3]), where $\chi = \log_{10} \frac{A}{m}$, see Figure 9. This page is activated only for catastrophic events, which are obtained for a large mass of the impact projectile and a large collision velocity. The page shows:

- First row: Histograms of size, area-to-mass ratio and Δv ;

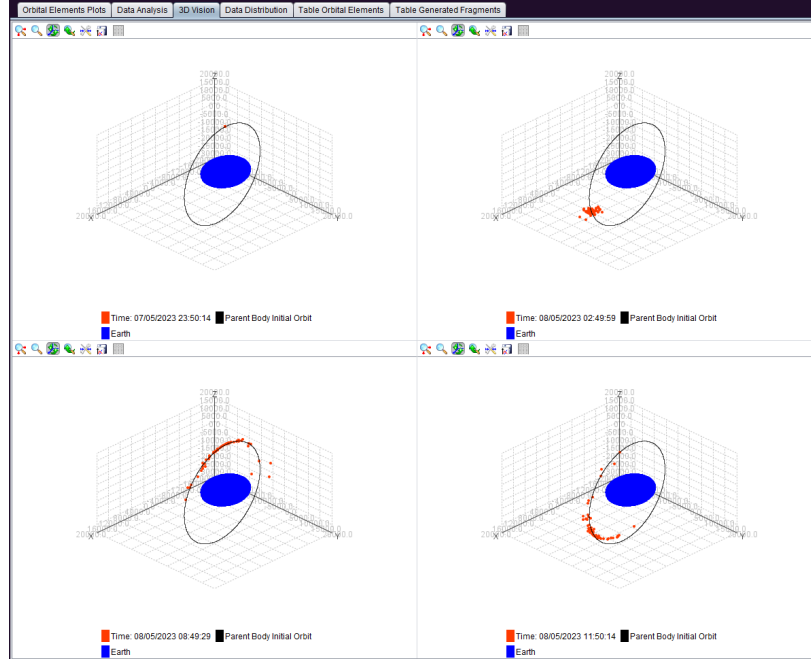


FIGURE 8. 3D plots.

- Second row (only for catastrophic events): Histograms of χ for the generated data and for different values of L_c versus the theoretical Probability density function (PDF) of χ .

3.7.5. *Table of Orbital Elements.* This page gives the data about the orbital position ($a, e, i, M, \omega, \Omega$), the area-to-mass ratio, the dimension, and the ID sequence number of each generated fragment after the break-up, see Figure 10.

3.7.6. *Table of Generated Fragments.* This page gives the state vector and the characteristics of each generated fragment after the break-up; the ID sequence number, the size, the area-to-mass ratio, the area, the mass, the delta velocity, the components of the velocity (V_x, V_y, V_z), the observation dynamical type, which could be elliptic or hyperbolic orbits, and escape or re-entry orbits, see Figure 11.

3.8. **Save Experiment.** To save the current experiment (including the evolution), press the button below the output text, see Figure 12.

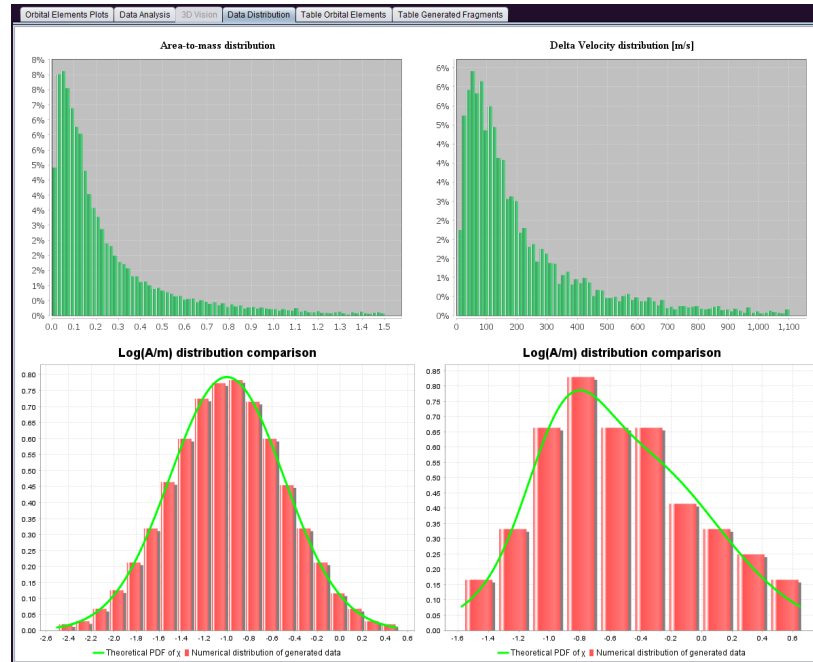


FIGURE 9. Data distribution window.

Semi-major axis (a)	Eccentricity (e)	Inclination (i)	Mean anomaly (M)	Argument of perig.	Longitude of node	Area-to-mass (A/m)	Dimension (d)	ID
20870.511918737	0.104177933512	61.710900305356	99.355785630240	50.388950933240	60.660826922487	0.164226760367	45.00	1
22569.714663864	0.171224104430	65.938654984447	63.585004447253	79.259961309397	59.089080540761	0.393407463753	30.00	2
21204.827742735	0.100925170727	62.203698695814	90.495770866025	59.332181433535	60.448208911386	0.112616802668	23.00	3
23700.052964525	0.108700554924	68.436358838916	25.593845525215	130.65085463921	57.870735570882	0.754038850563	20.00	4
23148.075529212	0.154544369825	62.749483944917	53.659334313395	91.839431159690	60.263434955814	0.24160894257	17.00	5
22173.829047627	0.039313711323	62.945224096442	31.168878530572	195.023882299928	60.189046743583	0.707059532828	15.00	6
21229.610333760	0.085511536283	63.314544031705	91.111474908302	60.050703925184	60.050520576995	0.073600847598	14.00	7
23390.291738918	0.158367867604	61.768349559981	50.476360127126	94.939713772109	60.639405768928	0.313688519662	13.00	8
20680.167351988	0.130320208968	63.395257985128	99.156671196886	48.118183537097	60.020290451926	0.149226575217	12.00	9
21768.137852555	0.100404218160	63.676677583108	75.589109140210	74.530247523927	59.915239834200	0.02022573246	11.00	10
21784.453130666	0.096989122422	63.226358417712	74.802500257432	75.581447859562	60.082714868777	0.03150051197	11.00	11
21336.095926250	0.106450418110	63.575308178319	86.468222196889	62.876934840052	59.953017385778	0.038424561935	10.00	12
21661.072243590	0.112201445636	63.844496164932	78.322981110993	70.400320003082	59.852851616160	0.051130784448	10.00	13
21852.22044431	0.098431771605	63.229917050401	73.351870983977	76.988444494102	60.082248455620	0.028408710181	9.00	14
22020.068076216	0.085610705173	63.325674402110	67.337101977032	84.750672722315	60.046349191392	0.062894402326	9.00	15
21908.753193766	0.110398824267	63.682733956237	72.562812172360	76.494348020752	59.912984997467	0.047858881614	8.00	16
21107.925551102	0.093220731885	63.783084440111	94.379150295783	56.885329669366	59.875599773392	0.063864204601	8.00	17
22249.599526113	0.062602686700	62.748120715404	61.913410745069	89.623532884026	60.263948093039	0.099280057636	8.00	18
21625.795304886	0.073066690111	62.801062047075	79.003970654112	74.054565348912	60.243906274730	0.135570083293	8.00	19
21626.319793853	0.102925222422	63.181029121801	79.260279615141	70.413771983528	60.100625895758	0.024069382418	7.00	20
21257.589734458	0.095146099685	62.819519362689	89.565304218880	60.874908089888	60.236922541005	0.060745701582	7.00	21
21864.804865996	0.102865267300	64.678607301115	73.263969655338	76.801845143856	59.645630209668	0.108246997926	7.00	22
20053.291289134	0.111809815609	63.099798444222	123.086897601181	62.438878546360	60.131171066507	0.173389079191	7.00	23
19565.897187089	0.118458854092	62.508421011020	139.115823628540	14.208311103727	60.354961899973	0.271667009008	7.00	24
21963.287139894	0.100891220713	63.725380169662	70.13625345155	80.15475208138	59.897110840973	0.041381441223	6.00	25
22009.791519100	0.081887486114	63.942174527309	69.221678175515	81.438252688251	59.816625941397	0.055884999116	6.00	26
22278.724282731	0.101310007028	62.839424143131	62.733298906545	87.850481252674	60.061993743739	0.073253344478	6.00	27
22110.794050615	0.111127121989	64.453444189118	67.97527096490	81.340448850699	59.62804303921	0.092775852841	6.00	28
21628.06592581	0.10971348124	61.850194070405	74.413672465533	74.342072893799	60.069912052860	0.145685706779	6.00	29
22589.933915818	0.144480590909	62.236679212663	61.580007907360	83.995234148352	60.459846444223	0.217382468409	6.00	30
22459.925705322	0.066134603553	64.789737109406	43.758200466934	112.400843060968	59.504925120896	0.322751528875	6.00	31
21280.095811441	0.111180511170	64.090135228192	87.460761596208	61.449896564273	59.761873384062	0.063642370397	5.00	32
22114.127250715	0.090705164052	63.03063703803	66.301326868034	84.532372253249	60.157129021195	0.078191020323	5.00	33
22255.097096396	0.118997361571	64.131872248681	85.531722486816	82.98342081309	59.745454800429	0.092490595354	5.00	34
22673.575319443	0.124292883717	63.098267613563	57.586860305516	90.862934158149	60.131747149931	0.121408964529	5.00	35
22566.210374831	0.128621032532	62.730285059575	60.52122224454	87.070389556929	60.270709988819	0.130442144591	5.00	36
20636.487819021	0.07789482559	63.13786295104	115.113540588779	38.423381422066	60.116844716256	0.182705247858	5.00	37
23647.337758978	0.150877542810	63.851549572642	44.844381356091	102.689037102911	59.850233598589	0.228961845096	5.00	38
22189.813849711	0.086101406792	66.382978381627	62.279370345762	90.52733920706	58.931104990537	0.296088909624	5.00	39
24629.244008065	0.177959587081	66.250492720653	36.276014025304	111.153337272881	59.075041499845	0.403501608887	5.00	40
23528.017507265	0.196345915288	61.260964775548	53.051564062048	87.461685052211	60.835526707965	0.527900830350	5.00	41
20312.171947683	0.154455509176	57.445430045369	102.76092321898	41.235361908569	62.388152065880	0.628420011311	5.00	42
22575.092387572	0.114802439505	63.571888238322	58.055684899204	91.483882031248	59.954293123946	0.090141306048	4.00	43
22679.489095546	0.116133092574	63.313860478458	55.99047144681	93.588494208482	60.050776785566	0.102531597880	4.00	44
21375.059629300	0.073738508109	62.967934556928	88.052192984141	64.932880508189	60.180854852035	0.115768262525	4.00	45
21333.595141953	0.075661458624	64.080310095600	89.368030059624	63.597282908594	59.765504651998	0.129319529107	4.00	46
22401.888594962	0.085405582591	63.507165625462	55.527423231549	97.428763267326	59.978451649020	0.15102580188	4.00	47
23033.254165897	0.196658507841	63.356154581347	44.837811582011	107.187485404451	60.014765638317	0.158164334001	4.00	48

FIGURE 10. Table of orbital elements.

M. APETRII, A. CELLETTI, C. EFTHYMIPOULOS, C. GALEŞ, AND T. VARTOLOMEI

ID	Size	Area-to-Mass	area	mass	delta velocity	Vx	Vy	Vz	X	Y	Z
1	128.00	0.1258253...	0.91355975...	7.25666345...	46.7735136...	-42.53991795...	-5.96619002...	-18.50733743...	13462.530324...	-31555.27064...	-28154.63143...
2	83.00	0.13039122...	0.38234300...	2.92094476...	47.1031198...	36.33872361...	10.62812003...	-28.02479740...	14544.204887...	31327.70542...	-29285.14856...
3	64.00	0.13096501...	0.22764388...	1.63643801...	47.7754126...	-35.96383346...	30.55144866...	7.66637950...	13552.711059...	-31055.17795...	-27785.70026...
4	54.00	0.14902753...	0.16193473...	1.08605647...	48.3708010...	-19.03845574...	-43.75070121...	-7.99389886...	13784.016237...	-32073.42631...	-28010.45589...
5	47.00	0.15688847...	0.12250202...	0.77253159...	48.9502462...	6.25315666...	6.25223376...	47.70040022...	1391.8300525...	-31556.13222...	-27246.68485...
6	42.00	0.16845508...	0.09784468...	0.58693548...	49.5788928...	-23.66699551...	-39.71676007...	17.90304178...	13721.343030...	-32018.10709...	-27655.31985...
7	38.00	0.17899218...	0.08005735...	0.44720738...	50.1841767...	-25.56794327...	41.88715740...	10.49751491...	14396.523454...	-30989.39059...	-27756.87504...
8	35.00	0.18925078...	0.06788940...	0.35872721...	50.7466684...	-3.20554524...	43.37589722...	26.14345770...	14001.939919...	-30878.62085...	-27542.31539...
9	32.00	0.20242297...	0.05672606...	0.28025330...	51.4341967...	8.84715552...	-2.60162188...	50.60075100...	13924.574030...	-31509.13084...	-26994.74256...
10	30.00	0.20788698...	0.04984174...	0.23998146...	51.6991135...	-44.27210096...	6.26929287...	25.9222139...	13438.776134...	-31596.38105...	-27544.93790...
11	28.00	0.21217121...	0.04303960...	0.20456874...	51.920120...	7.73466104...	45.42786495...	23.02078310...	14151.987792...	-30850.48131...	-27572.79618...
12	27.00	0.21407573...	0.04035179...	0.18805396...	52.0374638...	-31.98773889...	-36.6045123...	18.57657981...	13607.237008...	-31375.37178...	-28150.58693...
13	25.00	0.21975407...	0.03458262...	0.15738968...	52.2862372...	41.46126604...	-34.47354244...	15.67931218...	14641.929905...	-31809.07013...	-27685.61483...
14	24.00	0.22254739...	0.03189522...	0.14318400...	52.418494...	-7.20333277...	51.46039955...	4.96982655...	13947.114496...	-30764.70093...	-27966.94581...
15	23.00	0.22549143...	0.02929254...	0.12975770...	52.5564483...	-20.5221820...	7.3360517...	47.82548972...	13764.482462...	-31372.88449...	-28556.68427...
16	22.00	0.22859912...	0.02676467...	0.11708127...	52.7005214...	42.84483221...	-5.57125712...	30.16986251...	14693.512830...	-31549.85476...	-28314.56643...
17	21.00	0.14571339...	0.02438148...	0.10864607...	48.0857018...	37.99317866...	8.22516175...	-38.30385954...	14586.916185...	-31360.65838...	-28288.97546...
18	21.00	0.42197654...	0.02438148...	0.05777923...	59.5741235...	-47.60896778...	-3.92261151...	35.59597721...	13393.015934...	-31527.24615...	-28988.97548...
19	20.00	0.23536468...	0.02210064...	0.09393785...	53.0088205...	21.56707442...	4.95844519...	47.32053093...	14341.017830...	-31568.87788...	-28557.98752...
20	19.00	0.14717772...	0.01944913...	0.13554453...	48.2578998...	-40.16075125...	26.55588358...	-3.78374277...	13495.156886...	-31109.26385...	-27945.76252...
21	19.00	0.43442988...	0.01944913...	0.04502036...	59.5216486...	-28.49319061...	28.61079508...	-44.27120495...	13955.177939...	-31081.02874...	-28507.04271...
22	18.00	0.14893375...	0.01789993...	0.1041258...	48.3543984...	15.64896747...	37.33574776...	26.44444413...	14206.481937...	-30961.45208...	-27938.18756...
23	18.00	0.44110790...	0.01789993...	0.04057548...	60.1047739...	10.46134035...	-42.80466726...	40.87670078...	14188.359947...	-32060.45292...	-27340.27193...
24	17.00	0.15026609...	0.01596200...	0.10522489...	48.4587488...	8.95566021...	3.34027983...	48.71383465...	13924.457402...	-31345.54287...	-27260.15068...
25	17.00	0.44813141...	0.01596200...	0.03561901...	60.2484693...	-48.37263631...	-34.38447126...	-26.47576828...	13382.543311...	-31807.84896...	-28263.90604...
26	16.00	0.11839887...	0.01413531...	0.11397444...	46.2029143...	12.84183616...	-33.03482764...	28.72530216...	1421.926195...	-31326.47481...	-28308.46833...
27	16.00	0.25164059...	0.01413531...	0.05617263...	53.7224909...	32.76450385...	41.69117017...	8.67827734...	14495.213062...	-30901.72441...	-27782.51482...
28	16.00	0.64541834...	0.01413531...	0.02189422...	64.8627224...	25.48665737...	-5.39764781...	59.40820399...	13995.175616...	-31547.47397...	-27086.14126...
29	15.00	0.11933904...	0.01241884...	0.10407191...	46.2767044...	-14.38080913...	-21.85161344...	38.17290011...	13848.688598...	-31773.11454...	-27377.34666...
30	15.00	0.25643360...	0.01241884...	0.04843297...	53.9256003...	-31.49773917...	1.75782626...	43.73526663...	13813.958590...	-31449.35052...	-27301.07116...
31	15.00	0.65495950...	0.01241884...	0.01893002...	65.0401605...	-32.98234096...	56.04054433...	1.57784389...	13933.570041...	-30704.89682...	-27879.19311...
32	14.00	0.12040631...	0.01081554...	0.09892543...	46.3985508...	-3.11269226...	-28.52734169...	36.40902027...	14093.209551...	-31864.66166...	-27401.53945...
33	14.00	0.26138743...	0.01081554...	0.04135983...	54.1406386...	-46.32602375...	24.45959609...	-13.67579557...	13411.607986...	-31138.08188...	-26808.17423...
34	14.00	0.66489516...	0.01081554...	0.01267728...	65.2449210...	58.36978873...	-12.782025...	-27.86661555...	14846.349623...	-31586.82885...	-28280.51092...
35	13.00	0.08997430...	0.00932239...	0.10261180...	43.7344528...	20.32577108...	16.06276015...	34.25349757...	14324.635225...	-31225.75106...	-28370.50547...
36	13.00	0.15853236...	0.00932239...	0.03888439...	48.9805422...	5.23643051...	48.45310253...	4.89039437...	14117.708465...	-32137.01441...	-27833.62005...
37	13.00	0.26715059...	0.00932239...	0.03489567...	54.3689854...	38.54329587...	34.52790271...	16.68006662...	14574.460408...	-30999.95730...	-27672.09063...
38	13.00	0.48057012...	0.00932239...	0.01399692...	61.1434648...	16.91644225...	-0.01409546...	57.06214563...	14277.881606...	-31261.27259...	-27118.32613...
39	13.00	1.01144714...	0.00932239...	0.00921689...	70.9559204...	44.41314630...	20.18639526...	-51.52402110...	14654.950509...	-31196.62885...	-28807.40377...
40	12.00	0.09040545...	0.00794035...	0.08783047...	43.7762874...	1.38164681...	43.78866777...	-1.76191617...	14026.951843...	-30873.64603...	-27915.96176...
41	12.00	0.16121449...	0.00794035...	0.04925335...	49.1611870...	9.47544241...	-38.80207790...	-27.09813029...	14175.853908...	-32020.48648...	-28272.41605...
42	12.00	0.27318155...	0.00794035...	0.02968621...	54.6122758...	-50.11509094...	-1.18229570...	21.66925505...	13398.648637...	-31489.80497...	-27603.67211...
43	12.00	0.40070779...	0.00794035...	0.01620226...	61.3836667...	48.6769958...	28.51437828...	24.19175752...	14713.435367...	-31082.42341...	-27669.07962...
44	12.00	1.02545622...	0.00794035...	0.00774324...	71.1513960...	-1.71620431...	-33.54908257...	-49.82834780...	14022.363908...	-31656.25819...	-28958.41907...
45	11.00	0.0240097...	0.00666937...	0.27787911...	33.5777012...	-15.03143473...	-29.28277500...	6.8401975...	13839.762833...	-31875.02125...	-27809.85992...
46	11.00	0.04311833...	0.00666937...	0.13598492...	37.785165...	-6.12150513...	-32.14235358...	18.89748614...	13961.952076...	-31032.87138...	-28159.98717...
47	11.00	0.06734843...	0.00666937...	0.09902785...	41.2724844...	-14.20538381...	38.61495768...	-3.24782950...	13851.094283...	-30943.60971...	-27945.37106...
48	11.00	0.09699997...	0.00666937...	0.06693972...	44.6683567...	20.82893428...	24.96727268...	30.56039607...	14332.879251...	-31131.06016...	-28318.92038...
49	11.00	0.14848162...	0.00666937...	0.04491714...	48.3431049...	-14.95866229...	-40.01451408...	-22.63154010...	13840.788873...	-32022.19032...	-28211.18844...
50	11.00	0.23083932...	0.00666937...	0.02886426...	52.8054931...	40.90476542...	3.98115990...	16.22753999...	14736.265026...	-31392.80271...	-27676.29947...
51	11.00	0.41646686...	0.00666937...	0.01600713...	59.4229555...	13.53995718...	-28.23133986...	-50.50430888...	14231.578377...	-31800.86246...	-28959.42882...
52	10.00	0.02240564...	0.00550040...	0.24661007...	32.0992991...	4.61492058...	16.44838775...	-28.25105391...	14106.185416...	-31698.99021...	-28286.62266...
53	10.00	0.03010375...	0.00550040...	0.14089192...	37.0206213...	8.37872001...	-15.05189786...	-32.79125762...	14106.800056...	-31879.18116...	-28350.51133...
54	10.00	0.05892704...	0.00550040...	0.09349534...	40.1849032...	28.19689874...	-15.59225235...	-20.87935417...	14432.575315...	-31742.13084...	-28187.14623...
55	10.00	0.08429213...	0.00550040...	0.06404412...	43.1618343...	-21.8741848...	36.65751150...	5.24554590...	13745.530143...	-30968.28401...	-27828.02447...
56	10.00	0.11871360...	0.00550040...	0.04644920...	46.2274673...	16.10968817...	28.78357710...	32.68589396...	14266.780931...	-31079.00504...	-28345.24094...
57	10.00	0.16970136...	0.00550040...	0.03244528...	49.6520395...	21.67151776...	-32.3381386...	44.613397614...	14343.085115...	-31505.54094...	-27289.02514...
58	10.00	0.26723406...	0.00550040...	0.02025446...	59.6626655...	24.62666614...	-30.36306300...	-5.86834324...	14654.330444...	-32000.30064...	-28669.86848...

FIGURE 11. Table of generated fragments.



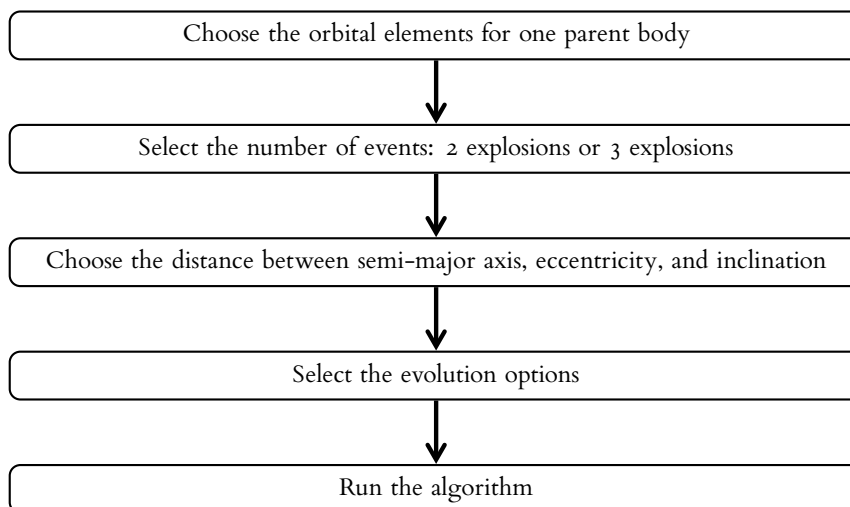
FIGURE 12. Save experiment button.

4. OPTION 2: GENERATE MULTIPLE BREAK-UP EVENTS

The first option of SIMPRO reproduces the break-up model Evolve 4.0 provided by NASA in [3] to generate two or three explosions and to analyze their evolution.

The work-flow is described in Section 4.1, the choice of the orbital elements is shown in Section 4.2, the selection of the number of break-up events is found in Section 4.3, while Section 4.4 shows how to get the evolution of the generated fragment on a given time interval, and Section 6.7 describes the different outputs generated by SIMPRO for multiple break-up events.

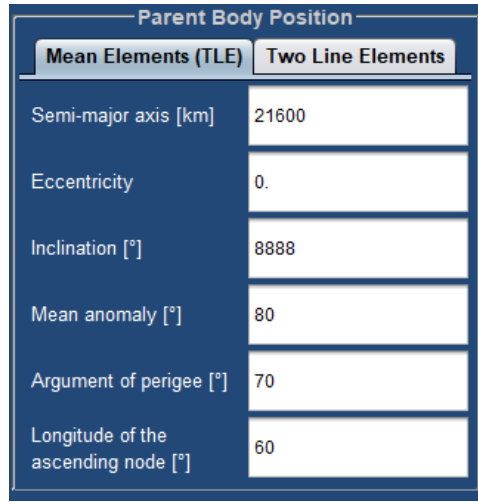
4.1. Work-flow. The work-flow below reproduces the left column that appears when opening SIMPRO for the second option of multiple break-up events.



4.2. Choosing Orbital Elements. Choose the orbital elements of the parent body (where the break-up event will happen), see Figure 1.

- Semi-major axis in km: $a > 6400$ km and $a < 45000$ km.
- Eccentricity $e \in [0, 0.75]$.
- Inclination in degrees: $i \in [0, 180^\circ]$.
- Mean anomaly in degrees: $M \in [0, 360^\circ]$.
- Argument of perigee in degrees: $\omega \in [0, 360^\circ]$.
- Argument of the ascending node in degrees: $\Omega \in [0, 360^\circ]$.

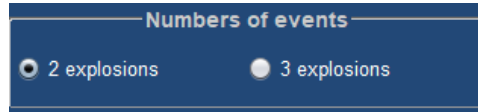
4.3. Number and Distance between Events. Select the number of break-up events, either 2 or 3 bodies (see Figure 14).



The screenshot shows a window titled "Parent Body Position" with two tabs: "Mean Elements (TLE)" and "Two Line Elements". The "Mean Elements (TLE)" tab is selected, displaying a table of orbital elements with their corresponding values in input fields.

Parent Body Position	
Mean Elements (TLE)	
Semi-major axis [km]	21600
Eccentricity	0.
Inclination [°]	8888
Mean anomaly [°]	80
Argument of perigee [°]	70
Longitude of the ascending node [°]	60

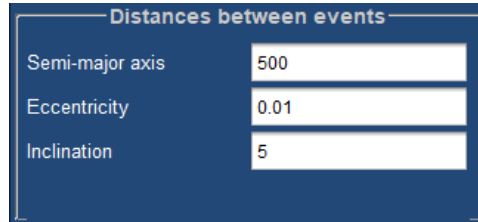
FIGURE 13. Choice of the orbital elements.



The screenshot shows a window titled "Numbers of events" with two radio button options: "2 explosions" (which is selected) and "3 explosions".

FIGURE 14. Selection of the number of break-up events.

Choose the distance in terms of a, e, i from the orbital elements of the first parent body (see Figure 15).



The screenshot shows a window titled "Distances between events" with three input fields for orbital elements: "Semi-major axis" (500), "Eccentricity" (0.01), and "Inclination" (5).

FIGURE 15. Distances of the orbital elements.

4.4. Fragments' propagation. To propagate the generated fragments, select Toggle activation with a LEFT CLICK and set the options with a RIGHT CLICK. One can choose "short-term" and "long-term" propagation, providing the period and step, the initial time and selecting the forces one wants to include in the propagation, namely the J_2 and J_3 terms of the geopotential, the effects of Moon and Sun, the Solar radiation pressure, and the drag effect due to the Earth's atmosphere, see Figure 16.

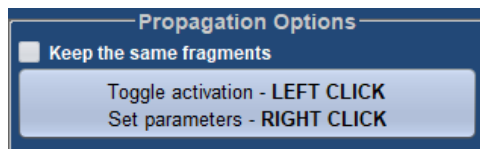


FIGURE 16. Propagation options.

4.5. Output. The output panel has two different frameworks, according to whether the orbits are propagated or not.

4.5.1. Orbital Elements Plots. The orbital elements a , e , i are plotted in the 2-dimensional planes of $a - e$, $a - i$, and $e - i$; Figure 17 shows the output without (left panel) and with propagation of the orbits (right panel).

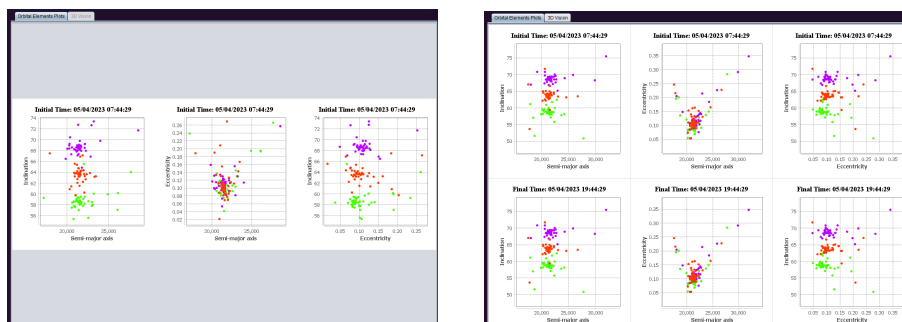


FIGURE 17. Plots of the orbital elements without and with propagation.

4.5.2. 3D Orbit Vision. This page allows to visualize the position of the generated fragments in a 3-dimensional space, whenever the propagation has been computed. An example is given in Figure 18 with the following description, where the blue dots make the contour plot of the Earth surface:

- Top-left: parent body position at break-up time.
- Top-right: fragments' orbits after 3 hours.
- Bottom-left: fragments' position after 6 more hours.
- Bottom-right: fragments' orbits after 3 more hours.

Each panel has additional options to zoom and move the graphs, rotate the plot, reset the zoom, modify the scale settings, save the picture, have a list of Cartesian coordinates (X , Y , Z) of each fragment at a given time, the coordinates of the parent body that gives the orbit, the coordinates of the blue dots representing the Earth. An option allows to decide whether visualize the fragments, parent body, and the Earth.

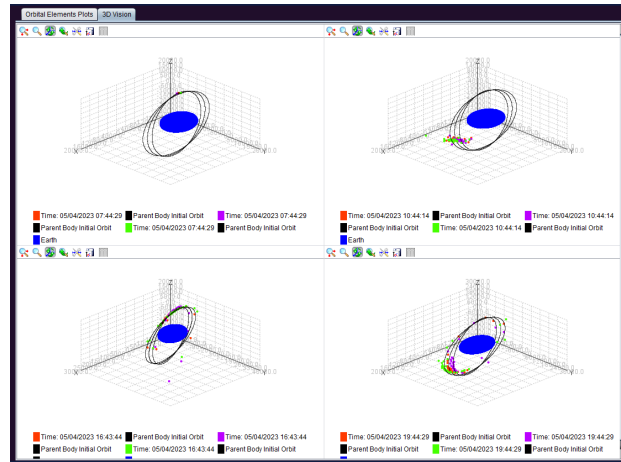


FIGURE 18. 3D plots.

5. OPTION 3: SAVED EXPERIMENTS

If an experiment is saved using Option 1, it can be retrieved using the third option, which allows one to see the elements and plots of the saved experiment, see Figure 19.

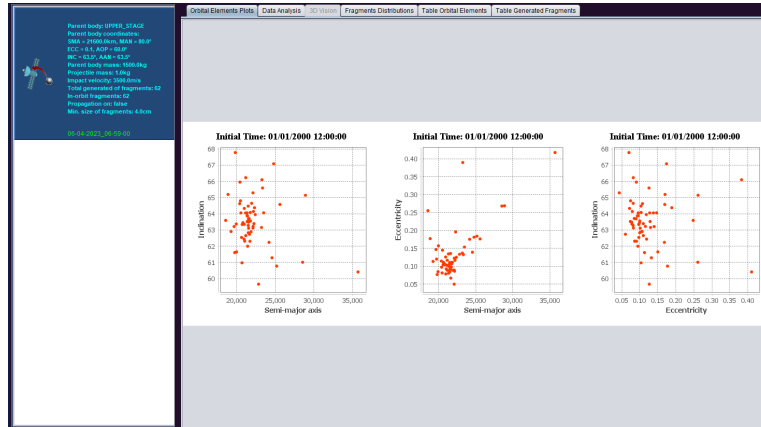


FIGURE 19. Saved experiments.

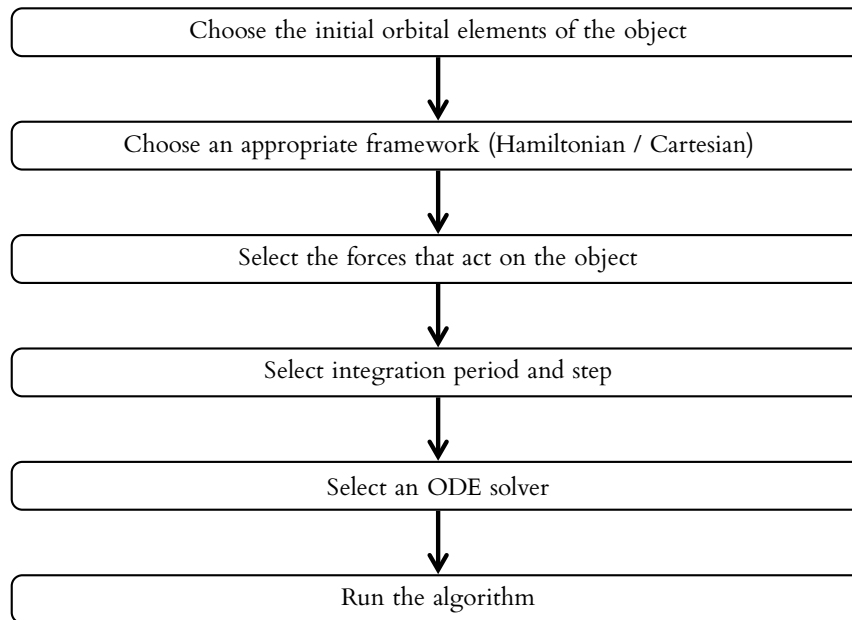
Pressing double click on one element on the left list will open the page from Option 1 using the input data of the selected experiment.

6. OPTION 4: ORBITS' PROPAGATOR

This option allows one to propagate the orbit of an object around the Earth, taking into account different forces.

The work-flow is described in Section 6.1, the choice of the orbital elements is given in Section 6.2, the selection of the forces is shown in Section 6.4, the selection of the framework, either Cartesian or Hamiltonian, is given in Section 6.3, the choice of the parameters is described in Section 6.5, the integration method can be chose as described in Section 6.6, Section 6.7 describes the different outputs generated by SIMPRO, while Section 6.8 gives the propagation history.

6.1. Workflow. This section reproduces the left column that appears when opening SIMPRO for the fourth option.



A summary of the equations and parameters used to propagate the orbits is shown when clicking on [Formulas - More Info](#), see Figure 20.

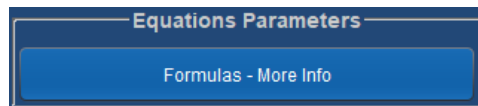


FIGURE 20. Equations and parameters for the propagation.

6.2. Choosing Orbital Elements. Choose **Mean elements (TLE)**, which allows to select the orbital elements to be propagated.

- Semi-major axis in km: $a > 6400$ km and $a < 45000$ km.
- Eccentricity $e \in [0, 0.75]$.
- Inclination in degrees: $i \in [0, 180^\circ]$.
- Mean anomaly in degrees: $M \in [0, 360^\circ]$.
- Argument of perigee in degrees: $\omega \in [0, 360^\circ]$.
- Argument of the ascending node in degrees: $\Omega \in [0, 360^\circ]$.

An example is given in Figure 21.

Equations Parameters	
Mean Elements (TLE)	Two Line Elements
Semi-major axis [km]	21600
Eccentricity	0.1
Inclination [°]	63.5
Mean anomaly [°]	80
Argument of perigee [°]	70
Longitude of the ascending node [°]	60
Area over mass	0.01
Initial Time	01/01/2000 12:00:00.0

FIGURE 21. Orbital elements of the parent body.

Alternatively, choose **Two Line Elements** and provide the data in LINE 1 and LINE 2 using the NORAD format from CelesTrak.

6.3. Selecting the framework. Select the framework to be used for the propagation of the orbits (see Figure 22).

- (1) For a long-period integration, select Hamilton's equations.
- (2) For a short-period integration, select Cartesian equations.
- (3) For a simplified perturbation model, select SGP4.
- (4) For a comparison between Hamiltonian and Cartesian propagation, select "Hamiltonian vs Cartesian".
- (5) For a comparison between Cartesian and SGP4 propagation, select "Cartesian vs SGP4".

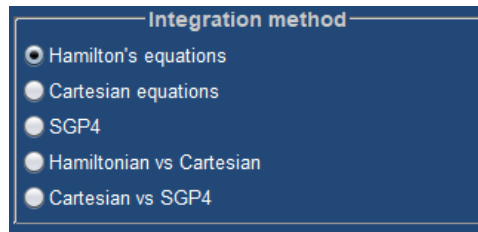


FIGURE 22. Selection of the integration framework.

6.4. Selecting the forces. Choose the forces that act on the object, among the following options (see Figure 23).

- (1) Geopotential: J2 and J3 effects.
- (2) Moon and Sun attraction.
- (3) Solar radiation pressure (for a given A/m).
- (4) Drag effect.

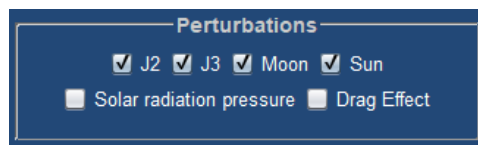


FIGURE 23. Selection of the forces.

6.5. Choosing the integration time and step. In the box shown in Figure 24, select the integration period in days and the integration step in minutes.

- (1) In case of Cartesian equations, it is convenient to select a time period between 1 day and 366 days with a time step of 1-5 minutes.
- (2) In case of Hamilton's equations, it is convenient to select a time period between 1 year and 500 years with a time step of 1-10 days.

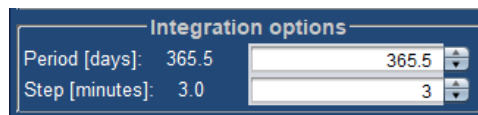


FIGURE 24. Select the integration options.

6.6. Choosing the integration method. In the box shown in Figure 25, select the integration method: Runge-Kutta or Adams-Bashforth-Moulton.

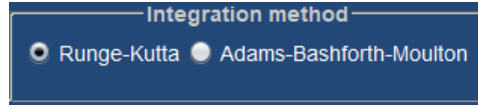


FIGURE 25. Integration method.

6.7. **Output.** The output of the integration consists in plotting the time evolution of the orbital elements $a, e, i, M, \omega, \Omega$, see Figure 27. For each run, one experiment page is created.

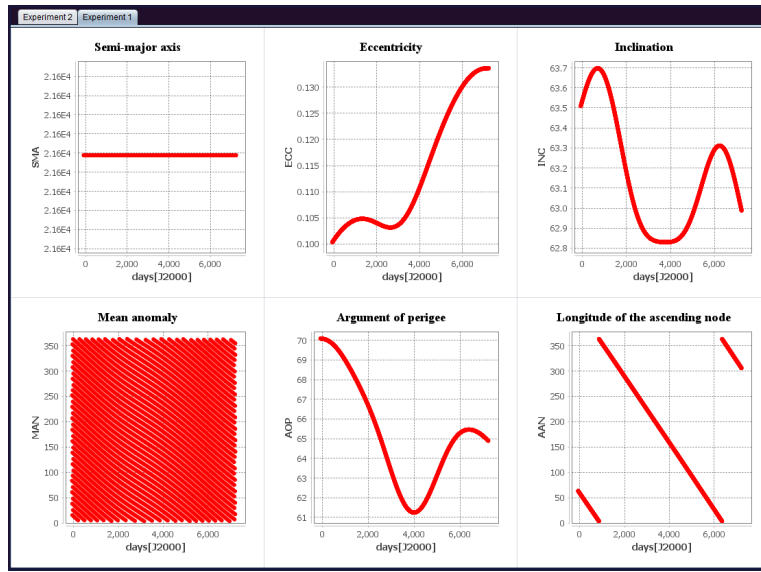


FIGURE 26. Output of the propagation.

6.8. **Propagation history.** The propagator stores up to 10 experiments on a single session (see Figure 27). Once the application is closed, all the experiments are erased.

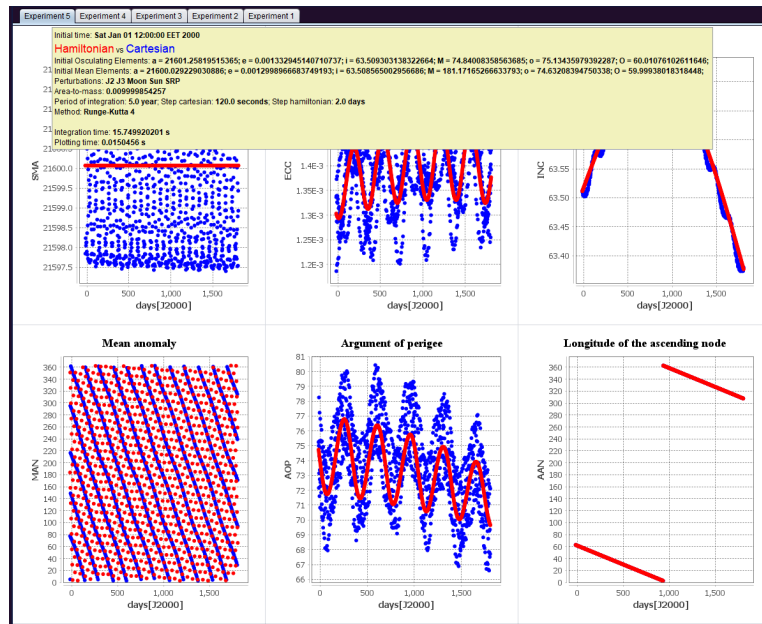


FIGURE 27. Different saved experiments.

7. OPTION 5: USER GUIDE PAGE

The option n. 5 allows the user to get access to an information page containing slides to illustrate graphically the overall program and each option, see Figure 29.

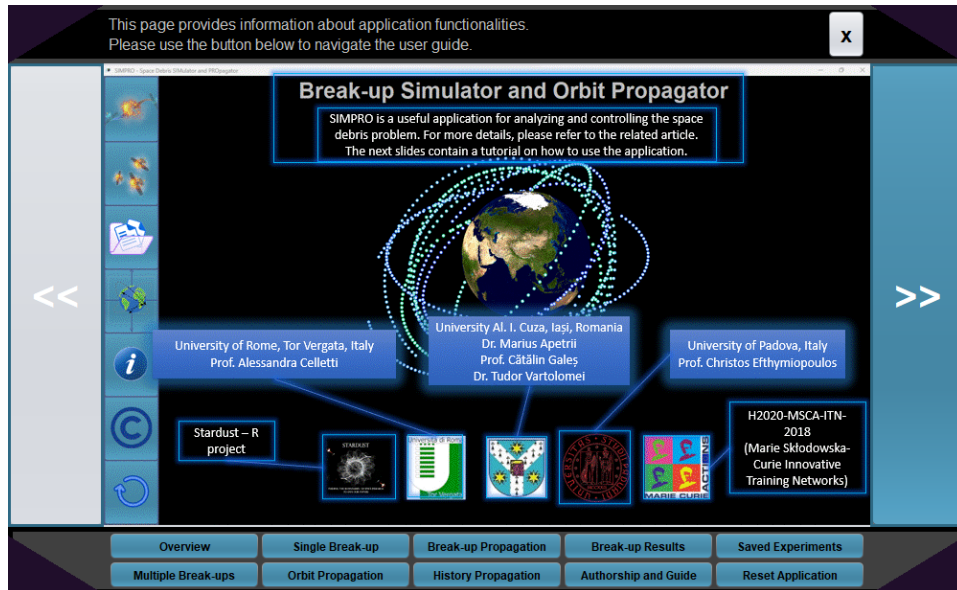


FIGURE 28. User guide page.

8. OPTION 5: COPYRIGHT PAGE

This page displays the detail of the related article and authorship of SIMPRO, see Figure29.



FIGURE 29. Copyright and contact page.

9. OPTION 6: RELOAD APPLICATION BUTTON

The last option reloads the program, removing any existing experiment from Option 1 and Option 2 and erasing all experiments from Option 4, see Figure 30.



FIGURE 30. The reload button.

REFERENCES

- [1] AAVV, *NASA Standard Breakup Model 1998 Revision*, prepared by Lockheed Martin Space Mission Systems & Services for NASA, July 1998.
- [2] M. Apetrii, A. Celletti, E. Efthymiopoulos, C. Gales, T. Vartolomei, *Simulating a breakup event and propagating the orbits of space debris*, Preprint (2023)
- [3] N. L. Johnson, P. H. Krisko, J.-C. Lieu, and P. D. Am-Meador, *NASA's new breakup model of EVOLVE 4.0*, *Adv. Space Res.*, 28, n. 9, 1377-1384 (2001)

DEPARTMENT OF MATHEMATICS, AL. I. CUZA UNIVERSITY, BD. CAROL I 11, 700506
IASI (ROMANIA)
Email address: mapetrii@uaic.ro

DEPARTMENT OF MATHEMATICS, UNIVERSITY OF ROMA TOR VERGATA, VIA DELLA
RICERCA SCIENTIFICA 1, 00133 ROMA (ITALY)
Email address: celletti@mat.uniroma2.it

DEPARTMENT OF MATHEMATICS, UNIVERSITY OF PADOVA, VIA VIII FEBBRAIO, 2, 35122
PADOVA (ITALY)
Email address: cefthym@math.unipd.it

DEPARTMENT OF MATHEMATICS, AL. I. CUZA UNIVERSITY, BD. CAROL I 11, 700506
IASI (ROMANIA)
Email address: cgales@uaic.ro

DEPARTMENT OF MATHEMATICS, AL. I. CUZA UNIVERSITY, BD. CAROL I 11, 700506
IASI (ROMANIA)
Email address: tudor.vartolomei@uaic.ro